Thermodynamics of Hydrogen Solution and Hydride Formation in Pd−Mn Alloys. 1. Disordered Alloys and a Correlation Effect

Ted B. Flanagan* and S. Luo

Chemistry Department, University of Vermont, Burlington, Vermont 05405

Received: October 26, 2005; In Final Form: February 28, 2006

The thermodynamics of H_2 solution and hydride formation/decomposition have been determined by reaction calorimetry (303 K) for disordered face centered cubic (fcc) Pd−Mn alloys. This alloy system belongs to the expanded lattice category which predicts that ΔH°_H and ΔH_{plat} for H_2 absorption should be more exothermic than those for Pd; the experimental results are that the former is more exothermic, at least at the higher Mn contents, but the latter is not. There is a regular decrease in the H capacity (at $p_{H_2} = 0.2$ MPa) with atom fraction Mn. A linear dependence of log p_{H_2} upon H content is found in the single hydride phase for all of these alloys suggesting that ΔH_H and ΔS_H are also linear functions of r in this region. This is confirmed using the $Pd_{0.875}Mn_{0.125}$ alloy which has no two-phase region (303 K). It is shown for the $Pd_{0.875}Mn_{0.125}$ alloy and for Pd that the changes of partial enthalpies and entropies with H content are correlated so as to minimize changes of μ_H.

Introduction

Kleppa and co-workers have employed reaction calorimetry with simultaneous measurements of the equilibrium p_{H_2} to determine the thermodynamics of H_2 solution in solid solution face centered cubic (fcc) Pd alloys at relatively high temperatures.[1] More recently Flanagan, Luo, and co-workers[2−4] have employed this same technique for several Pd-rich alloy systems but at moderate temperatures where the thermodynamic behavior is of more interest than at high temperatures because larger H contents can be reached and especially hydride phase formation and decomposition may take place. In these Pd-based systems, a hydride phase refers to a H-rich phase within the same metal atom sublattice as the dilute phase but with an expanded lattice, that is, Pd alloy−H systems have miscibility gap phase diagrams. The H atoms in both the dilute and hydride phases are disordered.

Several ordered phases exist in the Pd−Mn system, for example, Pd_3Mn and PdMn, but if quenched from an elevated temperature, fcc solid solution alloys are obtained. There is an increase of the fcc lattice constants of the Pd−Mn alloys with atom fraction Mn, X_{Mn}, but it is small compared to alloys such as Pd−Ag.[5] The Pd−Mn alloys, nonetheless, fall into the expanded lattice category relative to Pd,[6] and therefore values of ΔH°_H and ΔH_{plat} are expected to become more negative with an increase of atom fraction Mn, X_{Mn}, relative to Pd−H.[6] ΔH°_H and ΔH_{plat} are the relative partial molar enthalpies of solution of $(1/2)H_2$ at infinite dilution of H and the latter is an integral enthalpy change corresponding to

$$\frac{1}{2}H_2(1\ \text{bar}) + \frac{1}{(b-a)}MH_a \rightleftarrows \frac{1}{(b-a)}MH_b \qquad (1)$$

where a and b are the coexisting dilute and hydride phase boundaries and $M = Pd_{1-x}Mn_x$.

A calorimetric investigation of the reaction of H_2 with these alloys was carried out at elevated temperatures by Phutela and Kleppa[7] at low H contents where hydride formation does not occur. They found that ΔH°_H and ΔS°_H become increasingly negative with X_{Mn}; the latter was accounted for by assuming that H occupies only those octahedral interstices with Pd atoms as nearest neighbors which will be abbreviated as Pd_6. This is consistent with more recent results using neutron diffraction on the long-range superstructure[8] of Pd_3MnD_y and also on its $L1_2$ ordered form;[9] it was shown for the latter with $y = 0.7$ that only the Pd_6 interstices were occupied and, for the former with $y = 0.61$ that 85% of the interstices occupied were Pd_6.

Sakamoto et al.[6] determined ΔH° and ΔH_{plat} from pressure-composition-temperature (p-c-T) measurements for a series of Pd−Mn alloys up to $X_{Mn} = 0.10$ over a lower temperature range then used by Phutela and Kleppa. They found that ΔH°_H becomes more negative and ΔH_{plat} more positive with X_{Mn} which is unusual. No isotherms or details were provided.[6]

There have been several characterizations of H in ordered Pd_3Mn alloys,[10−13] but detailed thermodynamic results have not been given for H contents beyond the dilute phase for either the disordered or ordered forms of Pd_3Mn and alloys with $X_{Mn} < 0.25$. In this paper, Part 1, the thermodynamics of solution and hydride formation are given for disordered alloys, and in Part 2, the results for ordered Pd−Mn alloys will be given. Thermodynamic parameters for $X_{Mn} \leq 0.25$ will be determined here isothermally using a dual equilibrium isotherm-reaction calorimetric technique.

Experimental Section

The alloys were prepared by arc-melting and annealing the resulting buttons at 1133 K for 72 h in vacuo. The alloy buttons were then rolled into thin foil and reannealed. To obtain the disordered forms of alloys with $X_{Mn} \geq 0.10$, which undergo some ordering, alloy foils were quenched into ice water from the annealing temperature.

For reaction calorimetry, the alloys were cut into small pieces and mixed with about an equal amount of Cu powder as an aid in heat conduction. The twin-cell, differential heat-leak calo-

* To whom correspondence should be addressed. E-mail: flanagan@emba.uvm.edu.

10.1021/jp058277e CCC: $30.25
Published on Web 03/25/2006

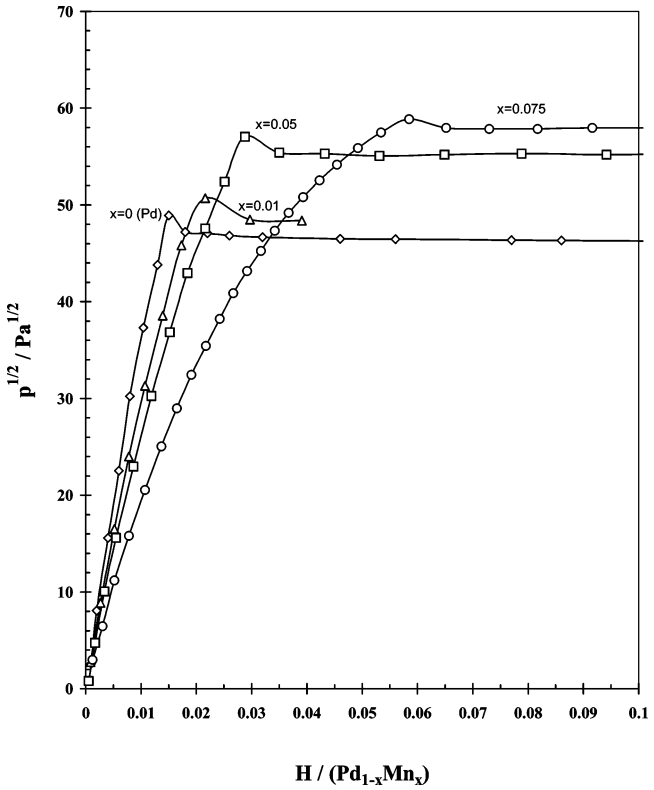

Figure 1. Dilute phase absorption isotherms (303 K) for annealed, disordered Pd−Mn alloys. The compositions, x, in $Pd_{1-x}Mn_x$, are shown on the isotherms.

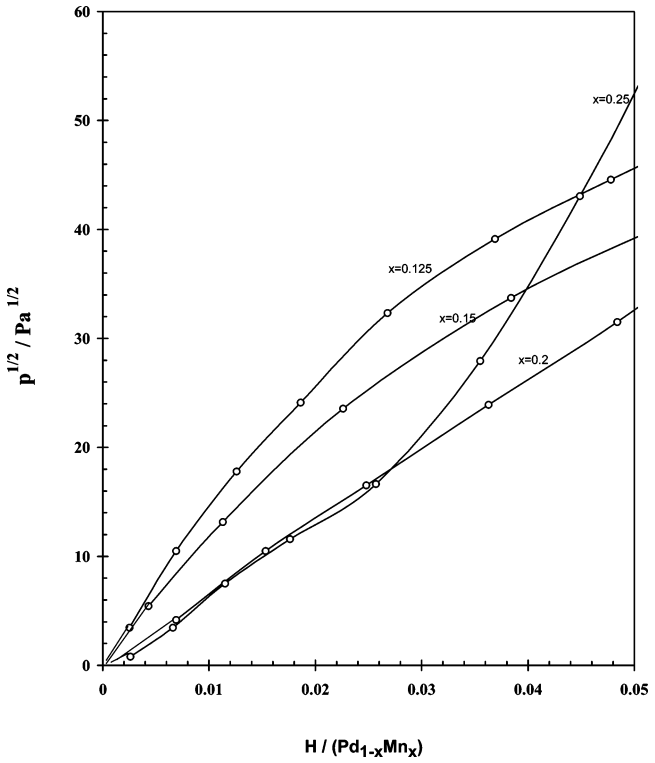

Figure 2. Dilute phase H_2 solubilities (303 K) for disordered Pd−Mn alloys which do not form a hydride phase. The compositions, x, in $Pd_{1-x}Mn_x$, are shown on the isotherms.

rimeter has been described elsewhere.[14] The heats released or absorbed during the reaction of H_2 are detected by the thermal imbalance of the two cells. The imbalance is quite small so that the calorimetry can be referred to as isothermal. Generally, the calorimeter was calibrated using the known heat evolved for H_2 absorption by Pd in its two-phase, plateau region. All of the calorimetric data were determined at 303 K.

The heats of absorption/desorption are determined using small increments of H_2 such that $(\delta q/\delta n_H)_T \approx \Delta H_H$. Simultaneous measurements of the equilibrium p_{H_2} and ΔH_H as a function of r allow the corresponding ΔS_H values to be determined. The calorimeter employed for part of this research is now capable of a greater precision than before[2−4] which is especially important for the dilute phase where the heats are small; data for the dilute phase of the $Pd_{0.99}Mn_{0.01}$, $Pd_{0.95}Mn_{0.05}$, and $Pd_{0.925}Mn_{0.075}$ alloys were determined with this greater precision (Figure 1), but the other data were determined before the modifications. The greater precision is not so important in the plateau and single hydride phases where the heats are greater.

Results and Discussion

H_2 Solubilities in the Dilute Phase. Dilute phase absorption isotherms are shown in Figure 1 at 303 K for the disordered forms of the $X_{Mn} = 0.01$, 0.05, and 0.075 alloys which have *not* been previously hydrided because the phase change introduces dislocations which affect the subsequent dilute solubilities.[15] It can be seen that the solubilities at a given p_{H_2} increase with X_{Mn} which must be due to ΔH_H becoming more negative with X_{Mn} in keeping with its expanded classification. If the only effect of increasing X_{Mn} were to be a smaller fraction of available interstices, then this would lead to *smaller* p_{H_2} which is contrary to the results (Figure 1). It can be seen that there is a supersaturation of the dilute phase for each of these annealed alloys. After hydride formation/decomposition (cycling), there is no longer any supersaturation as found for Pd−H.[15]

For those alloys which form hydride phases at 303 K, that is, $X_{Mn} = 0.01$ to 0.075, the terminal hydrogen solubilities, THSs, increase with X_{Mn} (Figure 1) where the THS is the dilute phase H content where the hydride phase first appears. Such an increase is expected since the THSs of *all* disordered solid solution fcc Pd-rich alloys increase with alloying.[6]

Figure 2 shows the dilute phase solubilities (303 K) for the disordered $X_{Mn} = 0.10$, 0.125, 0.15, 0.20, and 0.25 alloys which do not form hydride phases at 303 K. There is a solubility increase up to $X_{Mn} = 0.20$, however, the $X_{Mn} = 0.25$ alloy has about the same solubility at small p_{H_2} near the origin as the 0.20 alloy but behaves differently at higher p_{H_2} where it increases steeply with r resulting in a smaller solubility than the other alloys at higher p_{H_2}.

Complete Absorption Isotherms. Complete absorption isotherms up to ≈0.20 MPa (303 K) are plotted in Figure 3 as log p_{H_2} against r where each alloy is in its disordered form. It can be seen that after the transition from the two-phase to the single hydride phase region is complete or else, if there is no plateau, in the steeply rising portion of the relation, the log p_{H_2} against r plots are linear and can be expressed by

$$\log p_{H_2} = -A(T) + B(T)r \qquad (2)$$

This logarithmic relationship was first found by Wicke and Nernst for Pd−H,[16] and a plot for Pd−H employing data from the present investigation is included in Figure 3. It can be seen that the log p_{H_2} − r plots are all nearly linear with the slopes becoming steeper at $X_{Mn} \geq 0.20$.

Adherence to the logarithmic p_{H_2} relationship (Figure 3) means that ΔH_H and ΔS_H must also be linear functions of r in

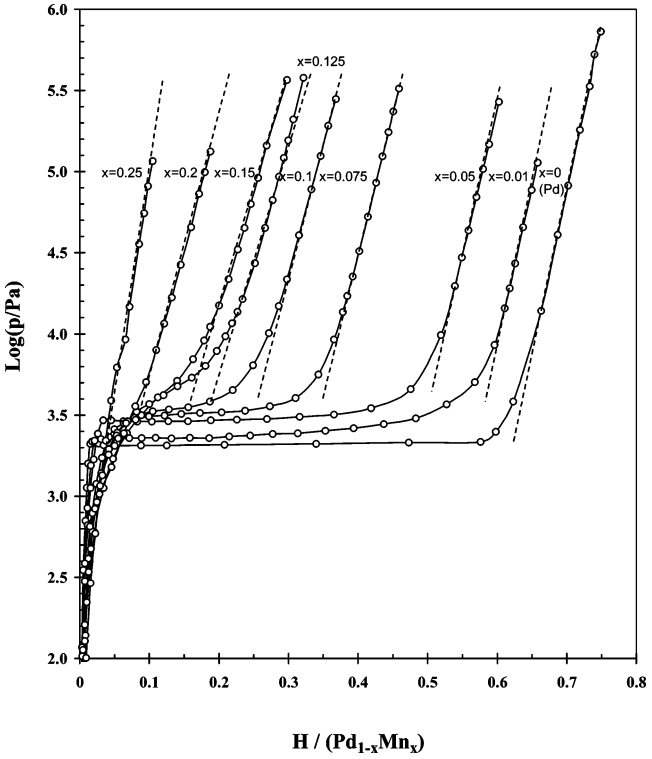

Figure 3. Absorption isotherms of log p_{H_2} against H/($Pd_{(1-x)}Mn_x$) for a series of Pd−Mn alloys (303 K). Dashed straight lines are drawn through the steeply rising portions.

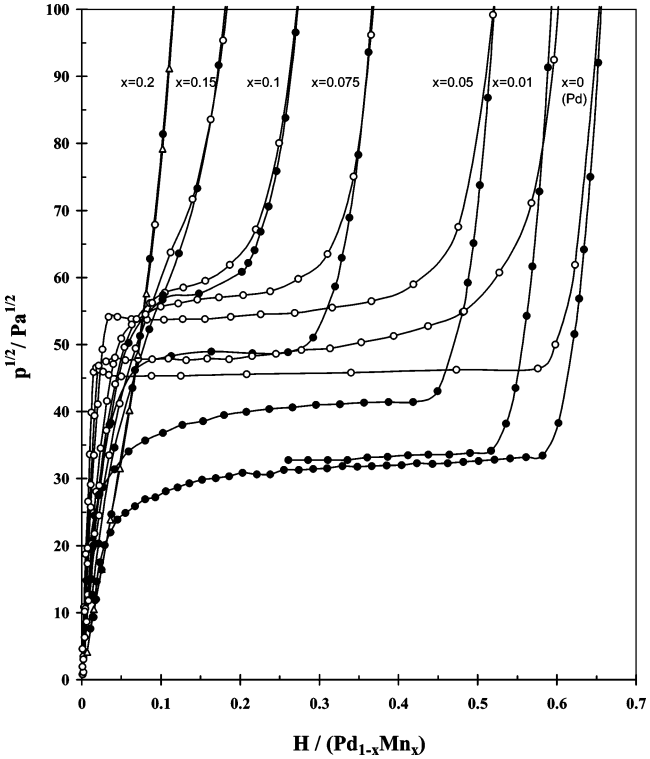

Figure 4. Absorption and desorption isotherms (303 K) for a series of disordered Pd−Mn alloys. The open and filled symbols are for the absorption and desorption of H_2, respectively.

this region or else one of them is, while the other is independent of r in view of the fundamental relation

$$RT \ln p_{H_2}{}^{1/2} = \Delta H_H - T\Delta S_H \qquad (3)$$

Desorption and absorption isotherms are shown in Figure 4 plotted as $p_{H_2}{}^{1/2}$ against r. If Figures 3 and 4 are compared, it appears that the log p_{H_2} against r plots (Figure 3) commence to be linear at the r value where the isotherms for absorption and desorption $p_{H_2} - r$ merge above the plateau at the upper phase boundary (Figure 4). This suggests that before the merging some dilute phase in the core is still being converted to the hydride phase.

Hysteresis is seen to be appreciable for the lower Mn content alloys and then it steadily decreases with X_{Mn} (Figure 4). It is surprising that there still appears to be some hysteresis for the $Pd_{0.90}Mn_{0.10}$ and $Pd_{0.85}Mn_{0.15}$ alloys which do not have two-phase regions (303 K).

If the average p_{plat} can be taken as $(p_f p_d)^{1/2}$ where p_f and p_d are the plateau p_{H_2} for hydride formation and decomposition, respectively, then these average plateau pressures increase with X_{Mn} but the increase is small suggesting only a small decrease of $|\Delta H_{plat}|$ with X_{Mn}. Values of $|\Delta S_{plat}|$ for all Pd alloys are usually close to that for Pd−H, 46 J/K mol H[3].

It is unusual for p_{plat} to increase with X_{Mn} while at a given H content in the dilute phase p_{H_2} decreases with X_{Mn} (Figure 1); this implies that $|\Delta H^\circ_H|$ increases and $|\Delta H_{plat}|$ decreases with X_{Mn}. Other examples where this occurs are the Pd−Zr[17] and Pd−Nb[18] alloys where, again, the expansion of lattice parameters and changes of thermodynamic parameters with X_M are small.

There is a decrease in the H contents with X_{Mn} evaluated in the high p_{H_2} region 0.2 MPa, however, the decrease is not linear especially at high X_{Mn}.

Calorimetrically Determined Enthalpies and Entropies. Dilute Phase. Reaction enthalpies were determined calorimetrically from the heats of reaction of H_2 with the alloys using small increments of H_2 as a function of the H contents of the alloys during both absorption and desorption. If small increments of H_2 are employed, then the enthalpies in single phase regions correspond closely to relative partial molar enthalpies, $(\partial\Delta H/\partial n_H)_{T,n_i} = \Delta H_H$. In the plateau region, the enthalpy change is an integral enthalpy corresponding to reaction 1.

TABLE 1: Enthalpies in Units of kJ/mol H and Entropies in Units of J/K mol H (with $\beta = 1$ for disordered Pd−Mn alloys (303 K))

X_{Mn}	ΔH°_H	$\Delta S^\circ_H(\beta = 1)$	ΔH_{plat}	ΔS_{plat}
0	−10.3	−55	−19.2	−45.0
0.010	−10.0(−10.2)[a]	−56.5	−18.9	−45.2
0.050	−10.9(−11.3)	−59.3	−18.3	−45.7
0.075	−11.2(−11.9)	−63.3(−56)	−18.5	−46.2
0.100	(−12.5)	(−58.5)	−18.2[b]	−46.1[b]
0.125	−12.8			
0.150	−12.5			
0.200	−15.0			
0.250	−15.5			

[a] The values in parentheses were determined elsewhere from p-c-T data,[6] and the others were determined in this research by reaction calorimetry. [b] Indicates that this alloy does not form a hydride phase, but the value has been determined from the enthalpy change of its "plateaulike region".

Thermodynamic parameters at infinite dilution of H are shown in Table 1 where the values in parentheses are from ref 6 and those without parentheses are from the present research by reaction calorimetry. It can be seen that $|\Delta H_H|$ increases slightly with X_{Mn}.

Equation 3 has been used to determine ΔS_H from ΔH_H and p_{H_2} as a function of r. The ΔS_H values were then employed to determine ΔS°_H at various r values using eq 5 with $\beta = 1$, and these were then extrapolated to $r = 0$ to obtain ΔS°_H at infinite dilution. The high-precision modification of the calorimeter was employed for the $Pd_{0.99}Mn_{0.01}$, $Pd_{0.95}Mn_{0.05}$, and $Pd_{0.925}Mn_{0.075}$

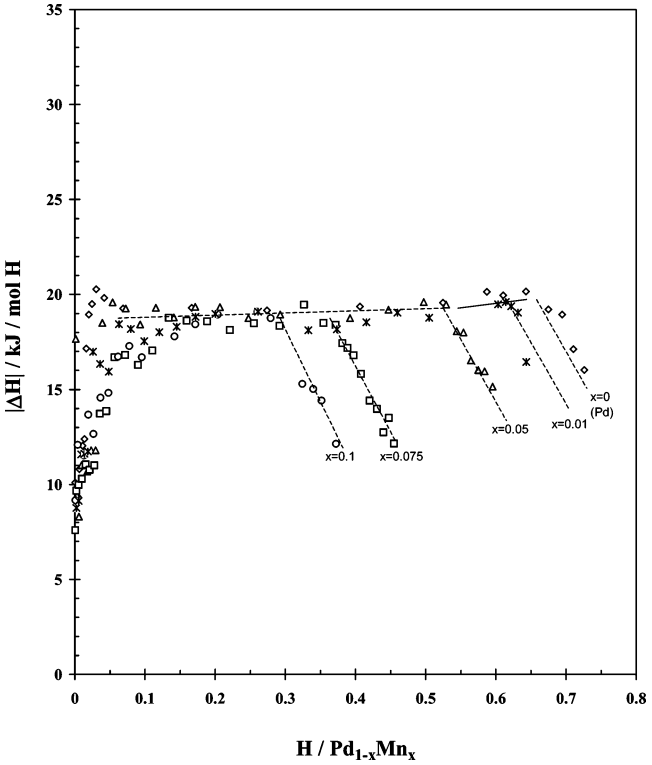

Figure 5. $|\Delta H|$ values for H_2 absorption for Pd−Mn alloys which form hydride phases at 303 K with the exception of $Pd_{0.90}Mn_{0.10}$: (◊) Pd; (×) $Pd_{0.99}Mn_{0.01}$; (△) $Pd_{0.95}Mn_{0.05}$; (□) $Pd_{0.925}Mn_{0.075}$; (○) $Pd_{0.90}Mn_{0.10}$.

alloys, and their thermodynamic values at infinite dilution should be reliable.

$$\Delta S_H = \Delta H_H/T - R \ln {p_{H_2}}^{1/2} \quad (4)$$

$$\Delta S^\circ_H = \Delta S_H + R \ln (r/(\beta - r)) \quad (5)$$

Since H atoms generally avoid interstices with Mn nearest neighbors,[7,8] the values of ΔS°_H are found to be more negative than that for Pd−H, −55 J/K mol H.[16,19] This suggests that β in eq 5 is <1, however, employing β = fraction of interstices surrounded by only Pd atoms, $f(Pd_6)$, from the binomial theorem, gives ΔS°_H values which are generally not as negative as the experimental values (Table 1).

Effects of Stress. It was noted above that the logarithmic relationship, $\log p_{H_2} = -A + Br$, is only obeyed at H contents above the p_{H_2} where the absorption p_{H_2} merges with the desorption p_{H_2} in the hydride single phase (Figure 4). This indicates there must be some dilute phase still being converted to the hydride phase in the region when p_{H_2} starts to increase from its plateau but before merging with the decomposition plot. This is verified by the ΔH_H values. For instance, absorption and desorption $p_{H_2} - r$ plots merge for the $Pd_{0.95}Mn_{0.05}$ alloy at $r \approx 0.51$ (Figure 4), and if the corresponding absorption ΔH_H values are examined, it can be seen that up to ≈0.51 they are still characteristic of hydride formation (Figure 5). The desorption values of $|\Delta H_H|$ in the single hydride phase region for, for example, the $Pd_{0.95}Mn_{0.05}$ alloy, are not characteristic of the plateau until $r \leq 0.45$ (Figure 4). This behavior is also apparent for the $Pd_{0.925}Mn_{0.075}$ alloy where the start of the linear falloff of ΔH_H with r characteristic of the single hydride phase starts at $r = 0.35$ coinciding with the merging of the absorption and desorption $p_{H_2} - r$ relations (Figure 4).

The sloping plateaux especially near complete hydride formation or complete hydride decomposition indicate that the simple phase rule, which assumes chemical equilibrium, is not obeyed in these regions of the plateaux where the core of the sample is the phase being converted and the outer part is the product phase. Compressive stress on the last fraction of dilute phase caused by the surrounding hydride phase would cause the gradual transition to the single hydride phase during absorption because the stress would increase the plateau p_{H_2} because increases of μ_H of the unreacted dilute phase core lead to an increase of μ_H by $+\sigma V_H$ and therefore of p_{H_2}. The gradual hydride → dilute phase transition (Figure 4) indicates tensile stress on the inner portions of the last hydride phase region to decompose and μ_H decreases by $-\sigma V_H$. Compared to these very gradual transitions, the transitions at the dilute/(dilute + hydride) and (dilute + hydride)/hydride phase boundaries are reasonably sharp, at least for the initial cycle, because they commence from the unstressed outer regions of the sample. If data for Pd−H(D) are examined,[14] then this is also observed. This effect of stress will be geometrically dependent because the core of unreacted material will differ with sample geometry. For example, the point where the absorption and desorption single hydride phase data merge is much closer to the absorption plateau for Pd black than for compact Pd.[20]

Plateaux Reaction Enthalpy and Entropy Values. Hysteresis is omnipresent in the two-phase region of metal−H systems, and this is reflected in the ΔH_{plat} values determined from van't Hoff plots but not in the calorimetrically determined enthalpies as discussed elsewhere.[14,21] Although reaction calorimetric enthalpy changes are unaffected by hysteresis, the entropy changes for reaction 1 for $p_{H_2} = 1$ bar are affected because either p_{plat} for absorption or for desorption can be employed resulting in different entropies. If, instead, an average plateau p_{H_2} is employed, then the role of hysteresis is minimized, that is

$$\Delta S_{plat} = \frac{\Delta H_{plat}}{T} - R \ln(p_f p_d)^{1/4} \quad (6)$$

It has also been shown that the entropies determined from van't Hoff plots should *not* be affected by hysteresis.[21] For Pd and its alloys, the entropy change for the plateau, reaction 1, determined from van't Hoff plots or from eq 4 has been found to be almost independent of the fraction and nature of M and $|\Delta S_{plat}| = 46 \pm 2$ J/K mol H.[3,14] Results for the Pd−Mn alloys are shown in Table 1 where the plateau entropies are close to this value.

ΔH_H against r plots are shown in Figure 5 for Pd−Mn alloys which *form* hydride phases (303 K) over the whole range of H contents accessible to $p_{H_2} \approx 0.2$ MPa and, to show that the trends are similar for alloys which do not form a hydride phase, the $Pd_{0.90}Mn_{0.10}$ alloy has been included. The $|\Delta H_{plat}|$ values do not appear to be very different from each other, but if the average values over the whole of the plateaux are calculated, they are slightly smaller than those for Pd (Table 1). The corresponding ΔS_{plat} values from eq 6 are shown in Figure 6 where there is seen to be a maximum in $|\Delta S_H|$ following the plateaux. The horizontal dashed line is the average value for Pd alloys of $|\Delta S_{plat}|$ which is close to the expected value of 46 J/K mol H[3].

Partial Enthalpies and Entropies at Higher H Concentrations. At the point where the absorption p_{H_2} merges with the desorption in the hydride single phase (Figure 4), the $|\Delta H_H|$ values for the alloys falloff nearly linearly with r (Figure 5). For pure Pd−H, or Pd−D, it appears that both ΔH_H and ΔS_H are also linearly dependent on r in the hydride single phase region.[14,23] Sakamoto et al.[23] have found a linear relation for Pd−H(D) between $\Delta H_{H,D}$ and r from 0.70 to 0.86; they were

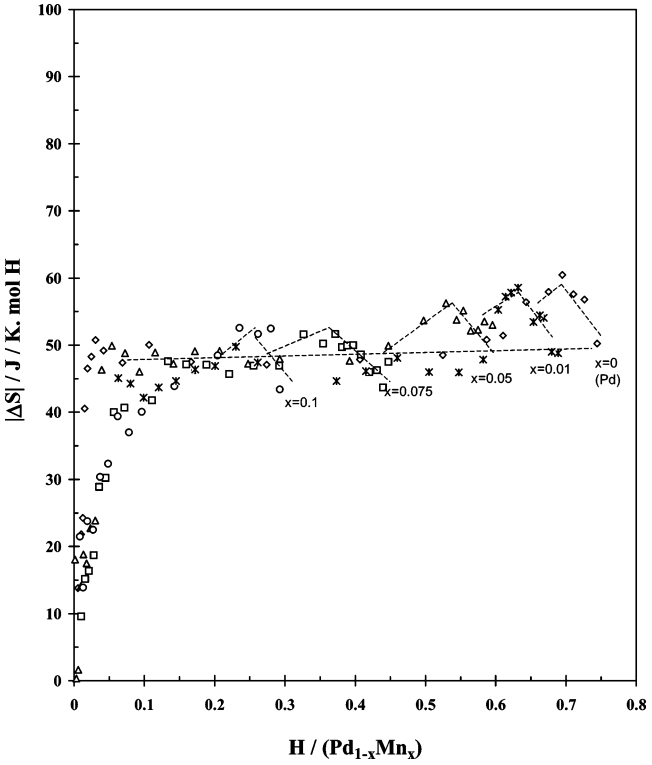

Figure 6. ΔS values for H_2 absorption for alloys which form hydride phases with the exception of $Pd_{0.90}Mn_{0.10}$: (◊) Pd; (×) $Pd_{0.99}Mn_{0.01}$; (△) $Pd_{0.95}Mn_{0.05}$; (□) $Pd_{0.925}Mn_{0.075}$; (○) $Pd_{0.90}Mn_{0.10}$.

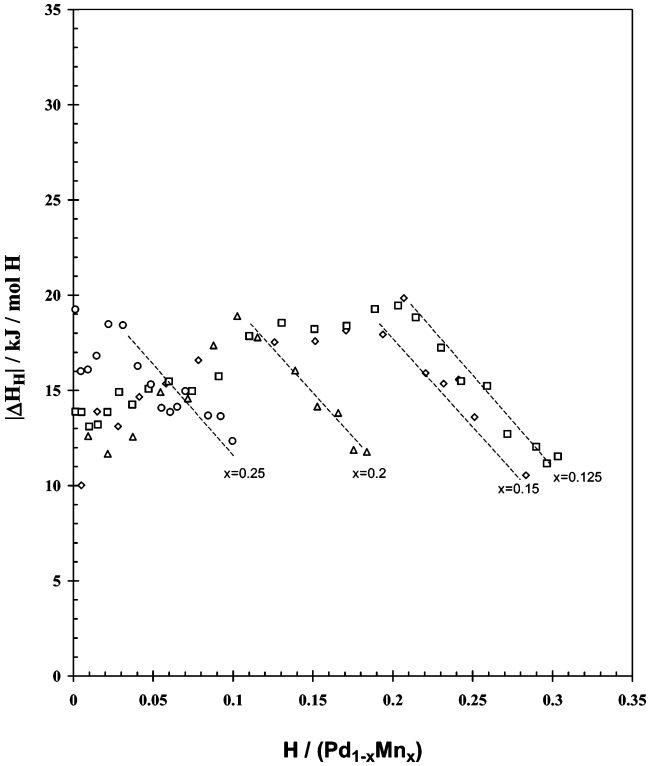

Figure 7. $|\Delta H_H|$ for H_2 absorption for alloys which do not form hydride phases: (□) $Pd_{0.875}Mn_{0.125}$; (◊) $Pd_{0.85}Mn_{0.15}$; (△) $Pd_{0.80}Mn_{0.20}$; (○) $Pd_{0.75}Mn_{0.25}$.

able to extend r to 0.86 by employing low temperatures ≤298 K where larger values of r can be reached for a given p_{H_2}. For some AB_5−H systems, ΔH_H and log p_{H_2} are also linear functions of r, for example, see Figure 2 in ref 24, and although it is not shown in ref 24, ΔS_H is also a linear function of r in that single hydride phase region.

A plot of ΔH_H against r is shown in Figure 7 for the Pd−Mn alloys which do *not* form hydride phases (303 K), and maxima are seen in the $|\Delta H_H|$ values which shift to lower H contents with increase of X_{Mn}. A linear region of ΔH_H against r can be seen for these in the single hydride phase region, and the slopes are similar to those which do form hydride phases; there is also linear behavior of ΔS_H with r in the same single hydride phase regions.

The $Pd_{0.875}Mn_{0.125}$ alloy is a good example of a Pd−Mn alloy which dissolves appreciable H but does not form a hydride phase (303 K) and where there are pronounced maxima in the plots of $|\Delta H_H|$ and $|\Delta S_H|$ against r for both absorption and desorption of H_2 (Figures 8, 9); the maxima in both figures occur at $r \approx 0.20$ which is close to the content where p_{H_2} starts to increase markedly (Figure 4).

Correlation between $|\Delta H_H|$ and $T|\Delta S_H|$. For pure metals, Gallagher and Oates[25] have shown that a correlation exists between ΔH_H° and ΔS_H°; the number of interstices per metal atom is allowed for in their correlation, for example, one for fcc and hexagonal close packed (hcp) and six for body centered cubic (bcc). This correlation effect is reasonable according to Gallagher and Oates, because the stronger the binding of the H in the metal lattice, the more negative will be both ΔH_H° and ΔS_H°. The former because of the stronger bonding and this causes the latter to decrease because the vibrational frequency of the H in the lattice will be expected to be higher, making ΔS_H more negative. This can be termed a thermal entropy effect with respect to this correlation.

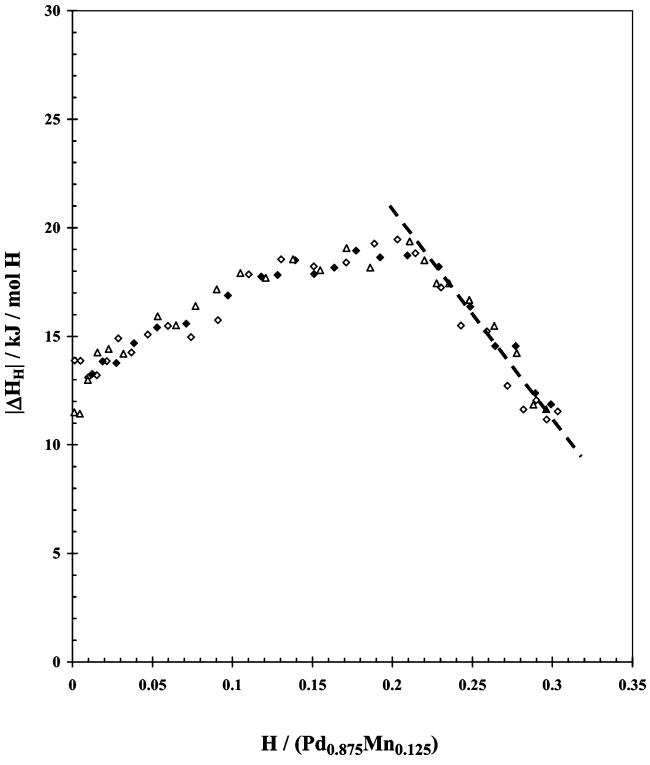

Figure 8. $|\Delta H_H|$ values for the $Pd_{0.875}Mn_{0.125}$ alloy (303 K) where the different symbols refer to different series of determinations: open symbols, absorption and filled symbols, desorption.

A different type of behavior was found for some Pd-rich alloys by Flanagan and Lynch[26] which has been extended to many Pd−RE alloys by Sakamoto et al.[27] and Weiss and co-workers also for Pd−RE alloys.[28] For these Pd−RE alloys, when ΔH_H° becomes more negative, ΔS_H° also becomes more nega-

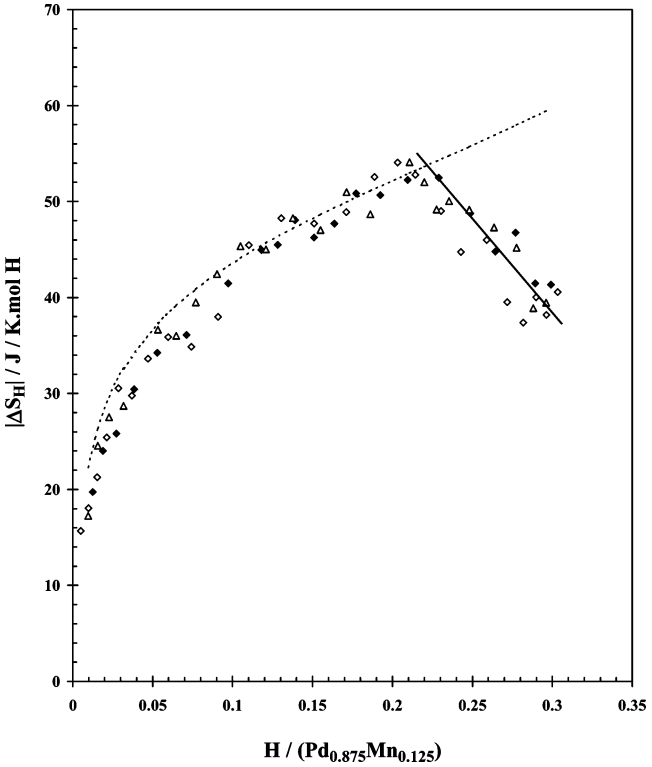

Figure 9. $|\Delta S_H|$ values for the $Pd_{0.875}Mn_{0.125}$ alloy (303 K) where the different symbols refer to different series of determinations: open symbols, absorption and filled symbols, desorption.

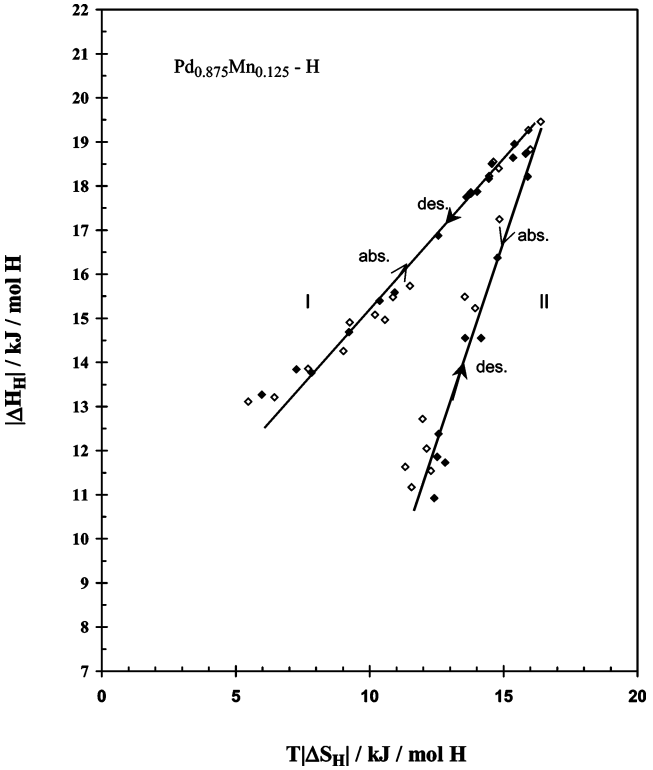

Figure 10. Correlations between $T|\Delta S_H|$ and $|\Delta H_H|$ for the $Pd_{0.875}Mn_{0.125}$ alloy. I refers to the region of H contents before and II refers to the contents after the maxima (Figures 8 and 9).

tive in keeping with the above trends but the slopes are much steeper than for the correlation made by Gallagher and Oates[25] and the reason for the correlations differ. These expanded Pd alloy correlation effects arise from the fact that the greater the atom fraction of RE, the more negative ΔH_H° will be and the greater X_{RE}, the more negative ΔS_H° will be because there are fewer Pd_6 interstices. There is a similar correlation for other expanded alloys such as Pd−Ag and Pd−Au as shown by Flanagan and Lynch.[26]

A collection of ΔH_H° and ΔS_H° values based on all the data available Pd-alloy systems up to 1995 are shown in Figure 7 of ref 6 where it can be seen that ΔS_H°(alloys, $\beta = 1.0$) < ΔS_H°(Pd) for almost all of the alloys. Both thermodynamic quantities decrease for the expanded alloys as mentioned above, but there is no trend for the contracted alloys except for the decrease of ΔS_H° with X_M.

In contrast to these correlations for Pd alloys and the pure metals, the correlations considered here between ΔH_H and ΔS_H are not due to the different pure metals[25] or to the metal solute concentrations in alloys[26−28] but to changes of H content for a given alloy composition. The $Pd_{0.875}Mn_{0.125}$ alloy has been chosen to illustrate this because it has no plateau (303 K) but, nonetheless, its H_2 solubility is appreciable (Figure 3). In Figure 10 $|\Delta H_H|$ is plotted against $T|\Delta S_H|$ for the $Pd_{0.875}Mn_{0.125}$ alloy where it can be seen that there is a linear relation between the two up to the maximum and then, at higher H contents, there is a correlation in the opposite sense between the two, that is, before and after the maximum, different correlations are obtained. Linear correlations between thermodynamic enthalpies and entropies for reactions have been reported many times for various types of reactions, for example, refs 29 and 30. When the two parameters change in a direction such as to cancel their effects, this is called a compensation effect, for example, for a given set of reactions if ΔH decreases, $-T\Delta S$ increases, such that ΔG itself does not change very much. The present correlations between $|\Delta H_H|$ and $T|\Delta S_H|$ cannot completely compensate each other, however, in view of the thermodynamic stability requirement that $(\partial\mu_H/\partial n_H) > 0$. The correlation found here is similar to a compensation effect but is not a complete one. Both absorption and desorption data follow the correlations. These are the experimentally determined relative partial quantities, and the partial entropies include the ideal and excess contributions. In both regions, the two partial quantities contribute to $\Delta\mu_H$ in opposing directions. The increase in $T|\Delta S_H|$ with r is the dominant factor in region I where the slope of the $|\Delta H_H|$ vs $T|\Delta S_H|$ plot is <1 (Figure 10) and >1 in region II. The partial enthalpy and entropy changes tend to compensate each other, but either one or the other dominates in each region.

The increase of $|\Delta H_H|$ in region I is partly due to an indirect H−H interaction which is the long-range elastic interaction due to the lattice expansion by H.[31] Mohri and Oates[32] have pointed out from the results of their cluster variation method calculations that there are also short-range interactions between H and vacancies on the interstitial sublattice which are of the same order of magnitude as the elastic long-range interaction. Thus, the dependence of the interaction energies on r arise from both the local arrangements of the H atoms in the sublattice and through the long-range elastic interaction. The increase of $T|\Delta S_H|$ with r in region I is mainly due to the ideal configurational entropy provided that it is calculated using $\beta < 1$ for the fraction of interstices occupied by H. The dashed curve in Figure 9 has been calculated by

$$\Delta S_H = -55 - R\ln(r/(0.52 - r)) \qquad (7)$$

where $\beta = 0.52$ has been chosen to fit the data and it is slightly greater than the fraction of Pd_6 interstices which is not unreasonable since some of the Pd_5 interstices are occupied in the long-period superstructure of Pd_3Mn.[8]

In region II, the slope is greater than 1.0 and therefore the decrease of $|\Delta H_H|$ with r (Figure 10) is the dominant factor

causing the strong increase of p_{H_2}, and μ_H, with r. The decrease in $|\Delta S_H|$ is due to positive contributions from the partial excess entropy, $S_H^E(r)$, because the ideal partial configurational entropy continues to increase with r in this region. The partial entropy is believed to be due mainly to nonideal configurational entropy terms.[33]

Although it has not been previously noted, similar correlations are obtained for Pd−H. The experimental situation is more complex for Pd−H because the partial thermodynamic data have to be obtained above the critical temperature and pressure, 563 K and $p_{H_2} = 19$ bar, and/or in single phase regions on either side of the two-phase envelope.[33] For Pd−H, the ΔH_H vs $T\Delta S_H$ correlations also have a greater slope after the maximum than before which is the same as the alloy, but the slopes for Pd−H are about twice those for the $Pd_{0.875}Mn_{0.125}$ alloy. For Pd−H, the maxima occur at $r \approx 0.50$ rather than 0.22 (Figures 8 and 9). The maxima in both the alloy and Pd correspond to approximately half-filling of the available interstices, that is, Pd_6, suggesting that at this point, H−H repulsive forces may become important as the average H−H distances become smaller in Pd−H. The situation is more complex in the alloy because of a combination of H−H repulsions and the preference of H for the Pd_6 interstices.

Conclusions

Hydrogen isotherms (303 K) and the accompanying thermodynamic parameters have been determined using reaction calorimetry for a series of disordered Pd−Mn alloys up to $X_{Mn} = 0.25$. The H capacities falloff with X_{Mn} although not as strongly as those for the Pd−Ag or −Au alloys. Values of $\Delta\mu_H(= RT \ln p_{H_2}^{1/2})$ increase linearly with r in the single hydride phase region for the alloys and for pure Pd. For alloys $X_{Mn} \geq 0.10$, $|\Delta H_H|$ and $|\Delta S_H|$ both increase and then decrease with r continuously and, for example, the maxima of the two parameters occur at about $r = 0.22$ for the $Pd_{0.875}Mn_{0.125}$ alloy. There is shown to be a correlation effect of $|\Delta H_H|$ and $|T\Delta S_H|$ with changes in r for the $Pd_{0.875}Mn_{0.125}$ alloy.

Acknowledgment. We wish to thank Dr. J. D. Clewley for valuable experimental assistance and also Professor A. Craft and Dr. H. Noh obtaining some of these data.

References and Notes

(1) Kleppa, O. *Ber. Bunsen-Ges. Phys. Chem.* **1983**, *87*, 741.
(2) Wang, D.; Lee, K.-Y.; Luo, S.; Flanagan, T. *J. Alloys Compd.* **1997**, *252*, 209.
(3) Zhang, W.; Luo, S.; Flanagan, T. *J. Alloys Compd.* **1999**, *293*−*295*, 1.
(4) Flanagan, T.; Luo, S.; Clewley, J. *J. Alloys Compd.* **2003**, *356*−*357*, 13.
(5) Raub, E.; Mahler, W. *Z. Metallkd.* **1954**, *45*, 430.
(6) Sakamoto, Y.; Chen, F.; Ura, M.; Flanagan, T. *Ber. Bunsen-Ges. Phys. Chem.* **1995**, *99*, 807.
(7) Phutela, R.; Kleppa, O. *J. Chem. Phys.* **1982**, *76*, 1525.
(8) Ahlzèn, P.; Andersson, Y.; Tellgren, R.; Rodic, D.; Flanagan, T.; Sakamoto, Y. *Z. Phys. Chem. N. F.* **1989**, *13*, 213.
(9) Onnerud, P.; Andersson, Y.; Tellgren, R.; Nordblad, P.; Boure, F.; Andre, G. *Solid State Commun.* **1997**, *101*, 433.
(10) Baba, K.; Niki, Y.; Sakamoto, Y.; Flanagan, T.; Craft, A. *Scr. Met.* **1987**, *21*, 299.
(11) Baba, K.; Sakamoto, Y.; Flanagan, T.; Kuji, T.; Craft, A. *Scr. Met.* **1987**, *21*, 299.
(12) Craft, A.; Foley, R.; Flanagan, T.; Baba, K.; Niki, Y.; Sakamoto, Y. *Scr. Met.* **1988**, *22*, 511.
(13) Flanagan, T.; Craft, A.; Kuji, T.; Baba, K.; Sakamoto, Y. *Scr. Met.* **1987**, *20*, 1745.
(14) Flanagan, T.; Luo, W.; Clewley, J. *J. Less-Common Met.* **1991**, *172*−*174*, 42.
(15) Luo, S.; Flanagan, T. *Scr. Mater.* **2005**, *53*, 1269.
(16) Wicke, E.; Nernst, G. *Ber. Bunsen-Ges. Phys. Chem.* **1964**, *68*, 224.
(17) Sakamoto, Y.; Miyagawa, U.; Hamamoto, E.; Chen, F.; Flanagan, T.; McNichol, R. *Ber. Bunsen-Ges. Phys. Chem.* **1990**, *94*, 1457.
(18) Sakamoto, Y.; Kajihara, K.; Kikumura, T.; Flanagan, T. *J. Chem. Soc., Faraday Trans.* **1990**, *86*, 377.
(19) Flanagan, T.; Oates, W. *Annu. Rev. Mater. Sci.* **1991**, *21*, 269.
(20) Frieske, H. Ph.D. Thesis, University of Münster, Münster, Germany, 1972.
(21) Flanagan, T.; Clewley, J.; Kuji, T.; Park, C.-N.; Everett, D. *J. Chem. Soc., Faraday Trans. 1* **1986**, *82*, 2589.
(22) Wicke, E.; Brodowsky, H. In *Metal Hydrogen Systems II*; Alefeld, G., Völkl, J., Eds.; Springer-Verlag: Berlin, 1978.
(23) Sakamoto, Y.; Imoto, M.; Takai, K.; Yanaru, T.; Ohshima, K. *J. Phys.: Condens. Matter* **1996**, *8*, 3229.
(24) Flanagan, T.; Luo, W.; Clewley, J. *Z. Phys. Chem.* **1993**, *179*, 35.
(25) Gallagher, P.; Oates, W. *Trans. Metall. Soc. AIME* **1969**, *245*, 179.
(26) Flanagan, T.; Lynch, J. *Trans. Metall. Soc. AIME* **1975**, *6A*, 243.
(27) Sakamoto, Y.; Kajihara, K.; Fukusaki, Y.; Flanagan, T. *Z. Phys. Chem. N. F.* **1988**, *159*, 61.
(28) Ramaprabhu, S.; Rajalakshmi, N.; Weiss, A. *Ber. Bunsen-Ges. Phys. Chem.* **1989**, *93*, 686.
(29) Grunwald, E.; Steel, C. *J. Am. Chem. Soc.* **1995**, *117*, 5687.
(30) Kreuzer, H.; Payne, S.; Grunze, M.; Wöll, Ch. *Z. Phys. Chem.* **1997**, *202*, 273.
(31) Alefeld, G. *Ber. Bunsen-Ges. Phys. Chem.* **1972**, *76*, 746.
(32) Mohri, T.; Oates, W. *J. Alloys Compd.* **2002**, *330*−*332*, 14−19.
(33) Kuji, T.; Oates, W.; Flanagan, T.; Bowerman, B. *J. Phys. F: Met. Phys.* **1983**, *13*, 1785.
(34) Luo, W.; Flanagan, T. *J. Phase Equilib.* **1994**, *15*, 20.
(35) Lynch, J.; Clewley, J.; Curran, T.; Flanagan, T. *J. Less-Common Met.* **1977**, *55*, 153.
(36) Luo, S.; Flanagan, T. *J. Less-Common Met.* **2002**, *330*−*332*, 29.